# Chemotaxis of Nonbiological Colloidal Rods

Yiying Hong,[1] Nicole M. K. Blackman,[2] Nathaniel D. Kopp,[2] Ayusman Sen,[1,2,*] and Darrell Velegol[2,3,*]

[1]*Department of Chemistry, The Pennsylvania State University, University Park, Pennsylvania 16802, USA*
[2]*Materials Research Institute, The Pennsylvania State University, University Park, Pennsylvania 16802, USA*
[3]*Department of Chemical Engineering, The Pennsylvania State University, University Park, Pennsylvania 16802, USA*

(Received 21 June 2007; published 26 October 2007)

Chemotaxis is the movement of organisms toward or away from a chemical attractant or toxin by a biased random walk process. Here we describe the first experimental example of chemotaxis outside biological systems. Platinum-gold rods 2.0 $\mu$m long exhibit directed movement toward higher hydrogen peroxide concentrations through "active diffusion." Brownian dynamics simulations reveal that no "temporal sensing" algorithm, commonly attributed to bacteria, is necessary; rather, the observed chemotaxis can be explained by random walk physics in a gradient of the active diffusion coefficient.

DOI: 10.1103/PhysRevLett.99.178103 PACS numbers: 87.17.Jj, 82.45.Yz, 82.65.+r

Chemotaxis is the movement of organisms toward or away from a particular chemical attractant or toxin by a biased random walk process. This phenomenon has been studied extensively since the 1880s, when Engelmann and Pfeffer discovered its occurrence in bacteria [1,2]. However, microscale chemotaxis has been reported previously only in biological systems [3–5]; sniffing robots [6] also chemotax, but they have an ~10 cm length scale. In this Letter we show experimental evidence of chemotaxis in a nonbiological system of bimetallic colloidal rods with hydrogen peroxide ($H_2O_2$) as the "attractant." We observed a random walk motion of 2.0 $\mu$m long platinum-gold (PtAu) rods in $H_2O_2$ solutions [7,8]. In a gradient of $H_2O_2$, the random motion of the rods appears to persist; however, the motion in fact has a slight bias directed toward higher $H_2O_2$ concentrations. Our observations are supported by Brownian dynamics simulations, which reveal that it is not necessary to have the "temporal sensing" mechanism commonly attributed to bacteria.

We have previously reported that PtAu colloidal rods become motile in the presence of aqueous $H_2O_2$ [7]. This non-Brownian motion is due to an electrokinetic mechanism resulting from the bimetallic redox catalytic decomposition of $H_2O_2$ occurring on both ends of the rods [7–9], and our rods are one of several possible types of "micro or nanoswimmers" [10,11]. The speed of the rods increases with increasing concentration of $H_2O_2$. On short time scales less than $1/D_r$, where for our systems the rotational Brownian diffusion coefficient $D_r = 1.0\ \mathrm{sec}^{-1}$, the motion is observed to be unidirectional. On time scales much longer than $1/D_r$, the direction of the motion appears random, giving a type of powered or "active diffusion" [12] from the combination of the electrokinetic propulsion and the rotational diffusion of the rods. The autonomous movement and the speed-concentration relationship prompted us to examine the possible chemotactic behavior of the bimetallic colloidal rods [11]. This directed movement is the first example of chemotaxis at the microscale observed outside a biological system.

The bimetallic colloidal rods (2.0 $\mu$m in length, 1 $\mu$m of each metal, and 370 nm in diameter) were synthesized by a previously reported method [13] and stored in deionized water for up to three weeks. We used two types of experiments to examine the motion (Fig. 1). In one setup [Fig. 1(a)], a concentration gradient of $H_2O_2$ was generated by placing an $H_2O_2$-soaked agarose gel [$\sim 1.0\ \mathrm{mm}(L) \times 1.0\ \mathrm{mm}(W) \times 0.5\ \mathrm{mm}(H)$] in the center of a 0.5 mm thick circular imaging chamber assembled on a glass cover slip. The chamber was then filled with the PtAu colloidal rod suspension in deionized water.

Upon filling the hydrogel with 30% aqueous $H_2O_2$ and adding the bimetallic rods, we observed a chemotactic response. The PtAu rods showed movement toward the gel, thus indicating the transport of rods up the $H_2O_2$ concentration gradient. After 110 h more than 70% of the rods were accumulated at the gel (Fig. 2). The change of PtAu rod number density at the gel is shown as the inset in Fig. 2. At this point the rods continued their active diffusion (due to the electrokinetic motion coupled with Brownian rotation of the rods), but they did not move away from the gel. Similar results were observed with 20% $H_2O_2$.

The speed of chemotaxis within the first minute of the experiment decreased from about 0.6 $\mu$m/s near the gel to less than 0.1 $\mu$m/s about 1.5 mm away from the gel. After an hour the chemotaxis speed near the gel decreased to less than 0.2 $\mu$m/s, with corresponding decreases farther out. The decreases in chemotaxis speed both with time and with distance are consistent with classical diffusion theory, which predicts that the $H_2O_2$ concentration gradient decreases with distance and time. Videos played at 30 times recorded speed reveal clear directional movements of the rods toward the gel [14].

Several control experiments were done to eliminate possibilities of nonchemotactic effects. The first control used noncatalytic monometallic Au rods in the same concentration gradient (gel soaked in 30% $H_2O_2$), while the second control used PtAu rods with no gradient (0%

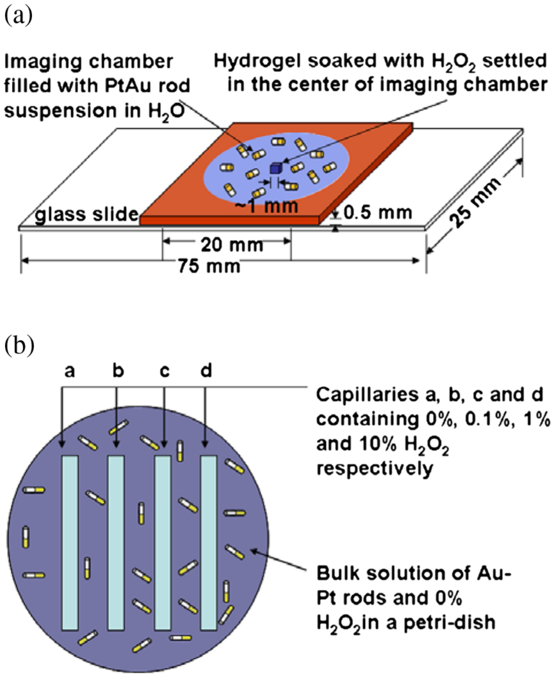

FIG. 1 (color online). Schematic of experiment setups: (a) Agar gel experiment. The gel contained 30% $H_2O_2$, which diffused into the bulk solution of PtAu rods in deionized water. The imaging chamber was sealed, and the movement of the rods was followed with a microscope. (b) Capillary experiment. The capillaries initially contained no rods but had various concentrations of $H_2O_2$ that diffused out. The outer suspension contained rods but no $H_2O_2$. The concentration of rods in each capillary was measured with time, to see whether the rods were chemotaxing into the mouths of the capillaries. A small rod concentration existed immediately outside the capillaries (wall thickness was 150 $\mu$m).

$H_2O_2$). Both types of experiments gave rod speeds that were mostly less than 0.05 $\mu$m/s and final rod distributions that were relatively flat with distance (i.e., missing the spike near 0 mm from the gel, which the experiments shown in Fig. 2 have). The monometallic Au rods did have finite speeds near 0 mm from the gel, although these were always less than 0.15 $\mu$m/s even at short times; these occurred due to inevitable asymmetries in the rods that occur during the electroplating process [7]. In a separate control experiment, polystyrene spheres initially concentrated near the gel were shown to diffuse away from the gel, indicating that the movement of the PtAu rods toward the gel was not simply due to a bulk flow.

A second type of experiment [Fig. 1(b)] was carried out using 2 cm long rectangular glass capillaries. These were filled by capillary action with 0%, 0.5%, 1%, and 10% $H_2O_2$ and capped at one end with wax. The capillaries were then placed into a polystyrene Petri dish containing a bulk solution of PtAu rods in deionized water with no $H_2O_2$. The setup is similar to that used by Pfeffer [2]. After 1 h the capillaries were removed and imaged along their 2 cm length. For the rods to enter the capillaries, they had to climb vertically, since the capillary walls are about 150 $\mu$m thick. Control experiments were done to assure that the removal process did not alter the distribution of rods within the capillaries.

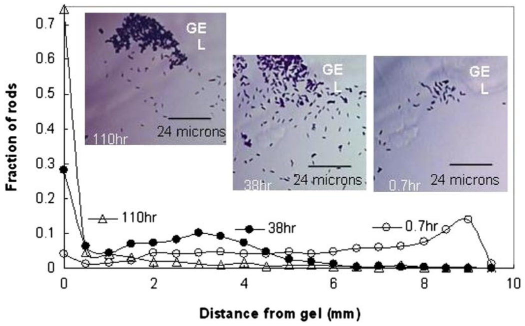

FIG. 2 (color online). The changing distribution of PtAu rods in a $H_2O_2$ concentration gradient. The gel (soaked in 30% $H_2O_2$) appears in the upper part. The images were taken at 0.7 h, 38 h, and 110 h. The fraction of rods was evaluated by dividing the number of rods in a frame at a certain distance by the total number of rods summed up from the frames at all the distances. Insets show the change in population of PtAu rods near the gel, visualized under bright field inverse microscopy at 50× magnification.

Figure 3 shows images of the four capillaries taken after 1 h. The diffusion of $H_2O_2$ out of the four capillaries created concentration gradients of varying strengths. As shown in Fig. 3(d), the highest concentration of rods after 1 h occurred in the capillary containing the highest initial concentration of $H_2O_2$. The concentration of rods through-

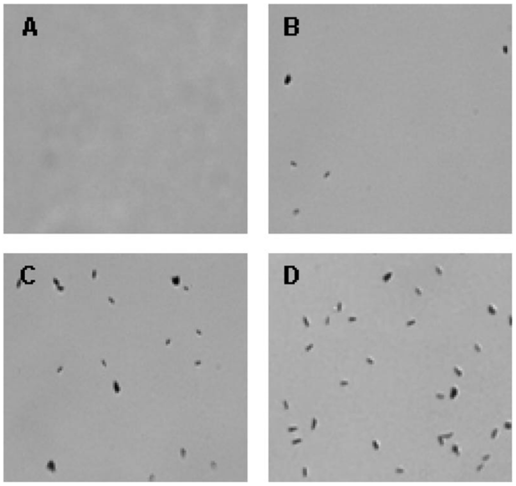

FIG. 3. Capillary experiments showing chemotaxis from bulk solution into the capillary. The capillaries initially containing (a) 0% $H_2O_2$, (b) 0.5% $H_2O_2$, (c) 1% $H_2O_2$, (d) 10% $H_2O_2$ seen after 1 h. An increase in the population of rods occurred with increasing initial $H_2O_2$ concentration. The images were taken at 40× magnification. Brightness and contrast were adjusted and cropping was done by Microsoft Office Picture Manager.

out the capillary was not uniform; it was highest near the capillary entrance, where the highest concentration gradient of $H_2O_2$ existed. It is important to recognize that while the concentration of rods was fairly high at the polystyrene Petri dish surface, the concentration of rods above the Petri dish at a height of $\sim 150\ \mu m$ (the capillary wall thickness) was nearly zero, since the diffusion height ($kT/\Delta\rho\pi a^2 Lg$) for the PtAu rods was less than $1\ \mu m$.

The mechanism of our rod chemotaxis is different from the "temporal sensing" mechanism commonly postulated for bacterial chemotaxis [5,15–18]. Temporal sensing implies an algorithm within the bacteria for knowing whether they are swimming up or down a gradient. For our bimetallic rods we propose simpler physics. The chemotaxis of our rods arises from their "active diffusion," which is caused by the combination of electrokinetic translation and the Brownian rotation (which makes the movement appear to be a random walk). A simple picture of the physics is that the rods move either up the gradient or down the gradient for the same finite amount of time ($\tau$), dictated by Brownian rotation. When the rods move up the gradient for a time ($\tau$), they move farther (increasing speed $U$, due to increasing concentration of $H_2O_2$) than when they move down the gradient for a time ($\tau$) (decreasing $U$). The net movement of the rod ensemble up the gradient gives the chemotactic response. In contrast to bacterial chemotaxis, for which directed bacterial "runs" (i.e., translation) have changes of direction due to "tumbles," the runs of our PtAu rods have changes in direction due to Brownian rotation. For bacteria, the frequency of tumbles is the primary parameter changing the effective "diffusion coefficient," but for our rods it is the change in $U$ caused by an increase in $H_2O_2$ concentration.

Brownian dynamics simulations (BDS) [19] were used to examine this proposed mechanism in more detail. The translation of rods from one position $\mathbf{x}(t)$ at a time ($t$) to $\mathbf{x}(t + \Delta t)$ in a small time step ($\Delta t$) is given by

$$\mathbf{x}(t + \Delta t) = \mathbf{x}(t) + \mathbf{U}\Delta t + \Delta\mathbf{x}(\Delta t), \tag{1}$$

where $\mathbf{U}$ is the translational velocity and $\Delta\mathbf{x}(\Delta t)$ represents the Brownian motion of the rod. An analogous equation was written for rod orientation, which in our case has only a Brownian rotation component (no driven part). Because of gravity our rods lie near to the two-dimensional glass surface but do not adhere due to repulsive colloidal forces. We consider mainly what happens at the surface of our system, and so we followed only the $x$, $y$, and $\theta$ directions. This matches the experiments corresponding to Figs. 1(a) and 2. For Fig. 1(b) the rods must move vertically to reach the capillary mouth, but a small initial vertical component of the rod might occur due to Brownian rotation of the rod.

In order to assess the contribution of the $H_2O_2$ gradient to the velocity of the rods, a dimensionless form of Eq. (1) was used (only $X$ is shown since no gradient exists in $Y$):

$$X(\tau + \Delta\tau) = X(\tau) + (1 + \varepsilon X)\cos\theta(\Delta\tau) + \Delta X(\Delta\tau). \tag{2}$$

Here $X = x/L$; $Y = y/L$; $\tau = tD_r$; $L$ is the characteristic distance moved before turning ($L = U_0/D_r \sim 5\ \mu m$, in agreement with our experimental observations); $U_0$ is the known, local rod translational speed ($\sim$5–10 $\mu m/\sec$) due to electrokinetics at some chosen position $X_0$; the rotational diffusion coefficient $D_r = 1.03\ \sec^{-1}$ for our rods at 298 K [20]; and $\varepsilon = (U/U_0 - 1)/(X - X_0)$ represents the $H_2O_2$ concentration gradient. The time step ($\Delta\tau$) used in the calculations ranged from 0.01 down to 0.0001, and 0.01 was sufficiently small in most cases to converge to less than 1% error. Several thousands trials were usually run, often enough to get uncertainties below 1% and always below 5%. We ran experiments to measure $H_2O_2$ concentration profiles using an Amplex Red dye (sensitive to $H_2O_2$ concentration), but the slow time response ($\sim$30 min or more) of organic dyes makes useful measurements difficult. Thus, typical values for $\varepsilon$ were estimated from diffusion theory, using the model of diffusion from a surface into a semi-infinite region [21], $(c - c_\infty)/(c_0 - c_\infty) = 1 - \mathrm{erf}(x/\sqrt{4Dt})$. For a 30% solution near the gel, $\varepsilon$ ranges from roughly $\varepsilon < -0.1$ in the first seconds to $-0.01$ after 1 min, to about $-0.0001$ after 100 h. The true Brownian motion of the rods is small ($<30\ \mu m$) for 1 h, while the chemotaxis movement is measured in mm. However, the electrokinetic translational motion, coupled with the rotational Brownian diffusion, gives an active diffusion with a long-time diffusion coefficient of $D_{\mathrm{active}} = U^2/D_r$ (from scaling the equations and the coefficient "1" from our BDS). For our systems, this is typically $10^{-10}\ m^2/\sec$, 2 to 3 orders of magnitude higher than the true diffusion coefficient.

Analytical modeling gives the scaling for the rod chemotactic speed as $U_{\mathrm{net}} \sim \varepsilon U_0$, and the detailed BDS reveal that $U_{\mathrm{net}} = \varepsilon U/2$, where $U$ is the local directed rod speed. As the time increases, a larger variation in rod speed is seen, with the rods in the higher concentration gradient moving the fastest and having a directed motion toward the higher speed regions (i.e., higher $H_2O_2$ concentrations). Typical speeds for the directed motion ($U_{\mathrm{net}} = \varepsilon U/2$) are consistent with experimental observations. For example, near the gels at early times, we found $U_{\mathrm{net}} \sim$ 0.6–0.8 $\mu m/\sec$, quite consistent with the estimated $\varepsilon$ of just under $-0.1$ and a measured $U$ of 10 $\mu m/\sec$. Simplified models that include the diffusion of $H_2O_2$ and the net speed ($U_{\mathrm{net}}$) are in solid agreement with Fig. 2. For example, such a model predicts that at 38 h, 30% of the rods should be near $x = 0$, while at 110 h, 85% should be near $x = 0$. While our simplified model neglects the coupling that occurs between the directed chemotaxis motion and the random active diffusion, we expect that the simplified model provides a semiquantitative result.

We distinguish the chemotactic movement of the PtAu rods from other possible types of motion. (1) The net movement of our rods is not due to simple translational Brownian motion. The movement is several millimeters in the first 40 min, whereas Brownian motion indicates only $\sim(2Dt)^{1/2} < 0.1$ mm. (2) Nor is the movement of the rods primarily the random walk motion due to active diffusion. The distances are comparable, $(2D_{\mathrm{active}}t)^{1/2} \sim 1$ mm or less, but our experiments reveal a unidirectional rod velocity, clearly inconsistent with a random walk that favors no direction. In addition, since the random walk motion grows as $t^{1/2}$, it cannot explain the magnitude of the movements in our long-time experiments. (3) Simple diffusiophoresis, which causes only the directed motion of the rods in a chemical gradient, does not have the primarily random motion of our bimetallic rods with a directed motion superimposed on it. Moreover, the control Au rods in an $H_2O_2$ gradient do not undergo the directed motion, which would be expected if the phenomenon were diffusiophoresis.

A natural question is, "What is in it for the rods, from a thermodynamic viewpoint?" However, the chemotaxis response is not an equilibrium problem but a nonequilibrium thermodynamic effect [22]. Other nonequilibrium thermodynamic effects, such as Soret diffusion, can be difficult to explain and are still debated from a thermodynamic perspective [23], although the dynamic (thermophoresis) perspective is more certain [24].

We have shown that our bimetallic colloidal rods exhibit chemotactic behavior in the presence of $H_2O_2$ concentration gradients. Having colloidal-sized engines with the ability to obtain mechanical energy from an *in situ* chemical "fuel" provides an alternative to external power sources [25] (e.g., electric, thermal [26], magnetic [27]). Furthermore, the motion proceeds without the consumption of the PtAu rods themselves. The colloidal rods move up a fuel gradient through catalysis; a straightforward extension is movement toward or away from a signaling molecule—a promoter or an inhibitor of the catalytic reaction. This behavior provides a novel way to direct particle movement toward specific targets, even while allowing the rods to sample a large region of fluid by apparently diffusive motion.

The proposed mechanism for chemotaxis is related to a well-known result for directed motion when a gradient of diffusion coefficient exists [28], although our chemotaxis in fact results from active diffusion rather than Brownian diffusion. The chemotaxis problem described here appears to be related to certain predator-prey or pursuit-evasion problems examined in other fields [29,30]. It remains to be seen whether this mechanism for chemotaxis, which requires only active diffusional motion in a gradient rather than an internal temporal sensing algorithm, is adopted by some bacteria.

We gratefully acknowledge the support of the Penn State Center for Nanoscale Science (NSF-MRSEC No. DMR-0213623) and NSF-NIRT No. CTS-0506967 for this project.

*To whom correspondence should be addressed:
asen@psu.edu
velegol@psu.edu

[1] T. W. Engelmann, Pfluegers Arch. Gesamte Physiol. Menschen Tiere **25**, 285 (1881).
[2] W. Pfeffer, Untersuch. Bot. Inst. Tubingen **2**, 582 (1888).
[3] J. Adler, Science **153**, 708 (1966).
[4] U. Alon, M. G. Surette, N. Barkai, and S. Leibler, Nature (London) **397**, 168 (1999).
[5] H. C. Berg, Phys. Today **53**, No. 1, 24 (2000).
[6] http://www.nytimes.com/2006/08/12/technology/12interview.html.
[7] W. F. Paxton *et al.*, J. Am. Chem. Soc. **126**, 13 424 (2004).
[8] W. F. Paxton *et al.*, J. Am. Chem. Soc. **128**, 14 881 (2006).
[9] T. R. Kline *et al.*, J. Am. Chem. Soc. **127**, 17 150 (2005).
[10] R. Golestanian, T. B. Liverpool, and A. Ajdari, New J. Phys. **9**, 126 (2007).
[11] J. R. Howse, R. A. L. Jones, A. J. Ryan, T. Gough, R. Vafabakhsh, and R. Golestanian, Phys. Rev. Lett. **99**, 048102 (2007).
[12] U. Erdmann, W. Ebeling, L. Schimansky-Geier, and F. Schweitzer, Eur. Phys. J. B **15**, 105 (2000).
[13] B. R. Martin *et al.*, Adv. Mater. **11**, 1021 (1999).
[14] http://research.chem.psu.edu/axsgroup/supporting_information.html.
[15] D. B. Dusenbery, Biophys. J. **74**, 2272 (1998).
[16] J. Adler and W. W. Tso, Science **184**, 1292 (1974).
[17] P. Devreotes and C. Janetopoulos, J. Biol. Chem. **278**, 20 445 (2003).
[18] R. M. Macnab and D. E. Koshland, Proc. Natl. Acad. Sci. U.S.A. **69**, 2509 (1972).
[19] W. B. Russell, D. A. Saville, and W. R. Schowalter, *Colloidal Dispersions* (Cambridge University Press, Cambridge, England, 1989). Sections 3.5 and 3.6 outline how the BDS is obtained from the Langevin equation. Further description of the Langevin equation and active diffusion appear in Ref. [12].
[20] T. G. M. Van de Ven, *Colloidal Hydrodynamics* (Academic Press, New York, 1989).
[21] R. B. Bird, W. E. Stewart, and E. N. Lightfoot, *Transport Phenomena* (Wiley, New York, 2001), 2nd ed..
[22] S. R. de Groot and P. Mazur, *Non-Equilibrium Thermodynamics* (Dover, New York, 1984).
[23] S. Duhr and D. Braun, Proc. Natl. Acad. Sci. U.S.A. **103**, 19 678 (2006).
[24] J. L. Anderson, Annu. Rev. Fluid Mech. **21**, 61 (1989).
[25] W. F. Paxton, S. Sundararajan, T. E. Mallouk, and A. Sen, Angew. Chem., Int. Ed. Engl. **45**, 5420 (2006).
[26] R. Piazza, J. Phys. Condens. Matter **16**, S4195 (2004).
[27] H. Watarai, M. Suwa, and Y. Iiguni, Anal. Bioanal. Chem. **378**, 1693 (2004).
[28] D. Ermak and J. A. McCammon, J. Chem. Phys. **69**, 1352 (1978).
[29] R. Isaacs, *Differential Games: A Mathematical Theory with Applications to Warfare and Pursuit, Control and Optimization* (Wiley, New York, 1965).
[30] A. Maye, C. Hsieh, G. Sugihara, and B. Brembs, PLoS ONE **2**, e443 (2007). They examine the movement of flies around obstacles, combining both random and deterministic motion.